Joint Special Interest Group meeting between euspen and ASPE
Advancing Precision in Additive Manufacturing
Inspire AG, St. Gallen, Switzerland 2021
www.euspen.eu

Stereo camera based in-situ monitoring of L-PBF process stability by spatter detection

Daniel Brummerloh[1,2], Dennis Jutkuhn[1,3], Zheng Yang[4], Alexander Penn[2], Claus Emmelmann[3]

[1]*Fraunhofer Research Institution for Additive Manufacturing Technologies IAPT, Germany*
[2]*Institute of Process Imaging, Hamburg University of Technology, Germany*
[3]*Institute of Laser and System Technologies, Hamburg University of Technology, Germany*
[4]*Hexagon Technology Center GmbH, Switzerland*

Daniel.brummerloh@tuhh.de

Abstract
The stability and reproducibility of the melting process is a decisive factor for the quality of the printing process and the final part. Stereo-vision in-situ monitoring based on two high-speed cameras in combination with fringe projection is used to investigate the three-dimensional layer topography, process spatter and residue of the melting process of laser powder bed fusion (L-PBF) process. The stereo camera system provides intensity data and a depth map of the working plane. The depth map has a lateral resolution of 40 µm and a depth variance σ^2 of 3.76 µm. The stability of the printing process can be estimated by monitoring the development of spatter and residue. Both are undesired by-products of the L-PBF process, which can indicate the present melting conditions. By optimizing the process conditions and reducing the scrap rate of printed parts, manufacturing costs can be reduced. This paper proposes a method to localize and quantify spatter emitted during the melting process, by combining the obtained depth data and the raw intensity data. The proposed method is evaluated in the course of an empirical investigation, which consists of three experiments. Within the experiments, unsuitable process conditions are caused intentionally by process parameter variation. In a real-life situation, these impairing process parameters could have been caused by defective machine components or miscalibration, and would possibly remain undetected without the technical ability to reliably monitor process stability. By measuring concentration, size and shape of the emitted spatter, the change in process parameters could be quantified and detected successfully by the proposed method. Especially overheating of material due to high local energy input and the dependency on the size of exposed area could have been identified reliably.

Algorithm, in-process measurement, selective laser melting (SLM), topography

1. Introduction

Additive manufacturing has been successfully used in series production for years, yet these processes continue to be restricted by inconsistency in manufacturing quality. A major cause is the nonexistence of universally applicable process parameters. Transferability of process parameters between manufacturing machines and parts to be built might not be given. Data and in-depth knowledge regarding the processes could be used, to find parameters for each individual case. Also, process parameters that guarantee long-term robustness during production are an actual challenge. To overcome these limitations, technical solutions are needed that would allow for the permanent monitoring and consequently for the assurance of the process parameters. To ameliorate systemic limitations of additive manufacturing, various measurement techniques allowing for the direct or indirect measurement of different process parameters have been researched in previous work.

Moreover, integrated stereo camera systems have promising potential to research various process parameters and to provide effective in-situ process monitoring capabilities. In this paper, a method is proposed to measure Laser Powder Bed Fusion (L-PBF) process stability indirectly through the quantification of spatter. Spatter is quantified by a processing chain that is executed on depth data acquired by a high precision stereo camera system. The spatter detection method is then empirically tested and evaluated in the experimental phase.

2. Process stability assessment through spatter quantification

The method proposed in this paper allows for in-situ monitoring of process stability of the L-PBF process. The method is based on depth data acquired by a stereo camera system. More precisely, the depth data is used to detect, localize and quantify individual droplets of spatter to indirectly assess the present process stability.

Spatter consists of cooled metal droplets that are ejected due to material overheating and evaporation during the laser exposure of the L-PBF process. They are emitted above an overheated melting pool and land locally around and within the processing area, influenced by the gas flow direction and intensity present in the building chamber [1]. The development of spatter can be seen as an undesired condition of the melting process. In general, spatter can have negative effects on the melting conditions and the process stability: with spatter droplets located on the powder bed and exposed areas, the material deposition can be interfered with [2]. Spatter droplets, that have been fused to the underlying part, pose a fixated obstacle that could even damage the recoating mechanism [3]. Furthermore, the energy input provided by the laser might be insufficient to remelt any spatter droplets in the exposed areas, so the fabrication of later layers might suffer from part defects. Beyond these disadvantages in manufacturing, the development of spatter can be used as a well-suited indicator of the present process stability.

Figure 1 shows an intensity image I (left) of a powder bed after laser exposure. Three exemplary spatter droplets are marked. The example shows that a high variation of the visual appearance or rather the resulting imaging data can be obtained. The variation is the result of different shapes, sizes and altered illumination based on their relative position within the build plane. Because of the variation, spatter detection based on intensity data is difficult and failure-prone.

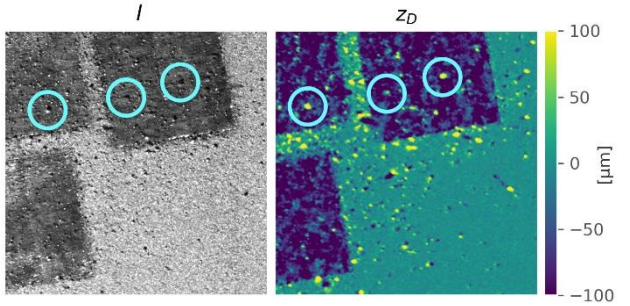

Figure 1. Monochrome intensity image I (left) of powder bed after laser exposure and resulting difference image z_D (right). Three exemplary spatter droplets are marked.

On the contrary, these variations are not to be observed within the depth data produced by the structured light system. Depth data is therefore more suitable for a robust detection algorithm. The right image of figure 1 shows a so-called difference image, that indicates change in topography caused by the laser exposure, see section 3.2. Individual spatter droplets are clearly visible in the form of a circular local maximum. Spatter droplets located outside the laser exposed areas also feature a preceding negative bump from the direction of its trajectory. This hollow is formed when the spatter droplets impinge on the powder bed surface. Examples of these pairs of local minima and maxima are marked with their approximate trajectory direction in figure 2. It should be noted that the spatter droplet trajectory can only be approximated right before impact. On the contrary, the origin and the initial trajectory cannot be determined, as the trajectory is not uniform under the influence of the laminar gas flow in the building chamber. Here, the gas flow is directed from the right to the left side in all the figures given in the paper.

By means of process stability monitoring through spatter detection, it is assumed that process accuracy and feasibility can be improved [4].

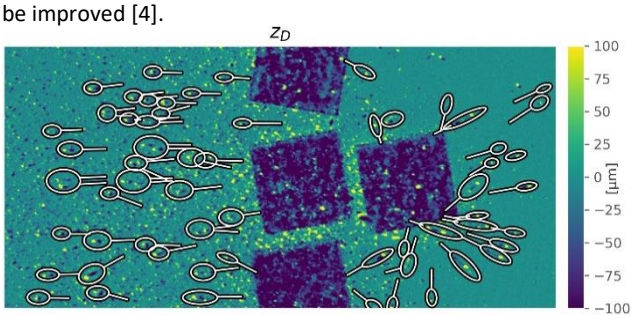

Figure 2. Difference image of depth data from exemplary depth map scan with approximated spatter trajectories.

3. Methodology

This section describes the complete process from data acquisition, over data processing to data evaluation. Additionally, the measurement hardware and its operating principle are being elaborated.

3.1. Acquisition of three-dimensional topography data

The depth data used to detect the spatter is acquired by a stereo camera system developed by Hexagon Technology Center GmbH. It consists of two high resolution monochrome cameras (7 920 × 6 004 pixels) with Scheimpflug adapter and a mechanical slide projector. Fringe projection is used to reconstruct a three-dimensional scene of the build plane [5, 6]. By using two cameras and various stripe patterns, redundant measurement data is collected to fully construct the depth information of the build plane, which has a size of 170 × 170 mm. Prior calibration is used to ensure a high level of precision.

During three-dimensional scene reconstruction, the system produces a three-dimensional triangle mesh with 32m polygons. However, such high resolution is not required to employ the spatter detection method proposed in this paper. Therefore, the triangle mesh is resampled into a uniformly structured depth map of 2 000 × 2 000 pixels resolution. The ability to deploy the method on the resampled resolution offers multiple advantages: the execution of the data processing runs at higher speed and the decreased amount of data allows for long-term storage to build up an extensive process knowledge database.

The accuracy of the system has also been examined within the scope of this work. Hereby, only the random error was examined by comparing repeated measurements. The systematic error is of little interest, as the method proposed in this paper is based on relative measurement change, i.e. systematic errors would sum to zero. The depth variance σ^2 was determined by calculating the difference in z-direction between sixty consecutive scans. The experiment had been repeated five times. The accuracy of the depth data provided by the structured light system was then determined to be σ^2 = 3.76 µm. The 95th percentile interval of the random error is bounded at 8.45 µm. The accuracy examination was based on the resampled depth maps of 2 000 × 2 000 pixels resolution.

Currently, the data acquisition and the data processing both take around 15 s respectively. The utilized system is a prototype that has not been optimized for operational speed yet, so both parts could be heavily optimized in the future. The operation potential of the structured light system in terms of speed is finally being discussed in section 6.

3.2. Difference Image

With two depth scans available, the change of the topography between two scans can be isolated by calculating their difference. To isolate emerging spatter, two scans are taken before $(t = t_0)$ and after $(t = t_1)$ laser exposure. The topography difference is calculated at each point (x, y) individually:

$$z_D(x, y) = z_{t_1}(x, y) - z_{t_0}(x, y)$$

As seen in figure 1, spatter droplets are clearly isolated and visible in the visualization of z_D.

3.3. Morphological operations

During the solidification of the material powder, the material exposed by the laser exposure gets compacted [2]. As a result, the surface level gets decreased by a small amount. This can also be seen in the depth data difference z_D in figure 2, as the quadratic, exposed areas show up in dark shades, indicating a negative shift.

The height normalization is performed with a morphological operation that is called reconstruction by dilation. During a normal dilation, high values replace neighbouring lower values. This spread of the highest values is then limited by maximum spread distance. Similarly, with the reconstruction by dilation, high values replace neighbouring lower values. However, the spread is not limited by distance but by a mask, which has to be specified as a second input to the operation. Thus, a reconstruction by dilation takes two inputs to produce an output image: a seed image and a mask image. The procedure is visualized in a one-dimensional example in figure 3.

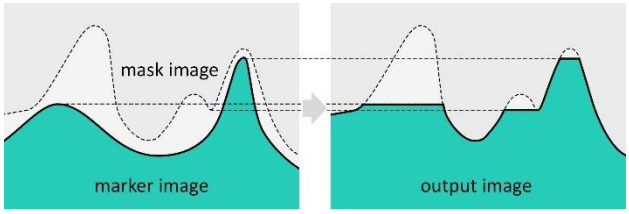

Figure 3. Qualitative functioning of the reconstruction by dilation in dependence of the chosen input image and mask image.

The algorithm used for the reconstruction is described in [7]. The desired normalization of the powder bed can be achieved by a special choice of seed image and mask image. In general, the values of the marker image need to be greater or equal to the values in the seed image. Within the scope of the proposed method, the mask image is chosen equal to z_D. The seed image is chosen as specified in the formula below. The seed image is also chosen equal to z_D except for the pixels along its contour Ω. The pixels in Ω are set equal to $\min(z_D)$ instead.

$$\begin{aligned} R_{\text{mask}}(x,y) &= z_D && \forall (x,y) \\ R_{\text{seed}}(x,y) &= z_D && \forall (x,y) \notin \Omega \\ R_{\text{seed}}(x,y) &= \min(z_D) && \forall (x,y) \in \Omega \end{aligned}$$

These rules for the deduction of mask and seed images have been applied in the example shown in Figure 4. In this specific case, $\min(z_D) = 2$.

Figure 4. Mask image and seed image deducted from an exemplary depth map z_D.

The result of the reconstruction by dilation z_R on a real-world depth scan z_D can be seen in figure 5 (middle). The normalized depth data difference $\tilde{z}_D$ can be calculated as follows. The result is visualized in figure 5 (right).

$$\tilde{z}_D = z_D - z_R$$

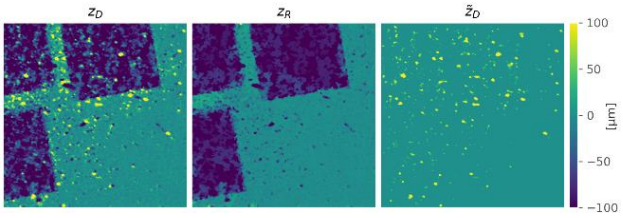

Figure 5. Difference image from depth data z_D (left), result of the reconstruction by dilation z_R(middle) and normalized difference image (right).

3.4. Spatter droplet segmentation

After the height normalization of the depth data difference image, spatter droplets are now isolated in $\tilde{z}_D$. More importantly, this applies both for spatter droplets within and outside the laser exposed areas in the powder bed. Individual blobs can be segmented by searching for connected regions with $\tilde{z}_D > 0$. For this labelling task, horizontal only connectivity is used. The utilized algorithm for region segmentation is described in [8].

3.5. Depth data cleaning

As with any measurement technique, the acquired depth data is subject to observational error. Very small droplets of spatter are hardly separable from signal noise. Fortunately, they are of little interest in the context of the process stability monitoring due to their little disturbing influence on the process**.** The data is therefore cleaned in such a way that small spatter droplets are excluded from the subsequent data analysis. The first step is to globally shift $\tilde{z}_D$ by 3 µm in negative direction.

$$\tilde{z}_{D,s}(x,y) = \tilde{z}_D - 3\mu\text{m}$$

By doing so, individual spatter droplets are separated more distinctively when the threshold $\tilde{z}_{D,s} > 0$ used for binary segmentation is applied. The resulting segmentation map S is visualized in figure 6 (middle). The shift of 3 µm has been determined empirically and depends on the depth data measurement accuracy, see section 3.1. As a third step, connected regions Φ_i or rather individual spatter droplets in with a size of 10 pixels or fewer are removed from the binary mask S. The threshold of 10 was also chosen empirically and with the relevance for the process stability monitoring in mind.

3.6. Volume Calculation

With the spatter droplets segmented, the droplets individual volume can now be quantified. The volume of each individual spatter droplet V_i is calculated by integrating the unshifted depth data difference image z_D over the area of the segmented spatter droplet Φ_i. V_i is shown in figure 6 (right).

$$V_i = \int_{\Phi_i} z_D \, \mathrm{d}A$$

It should be noted that this technique only accounts for the spatter volume located above the reference layer, which is defined by the powder bed before laser exposure.

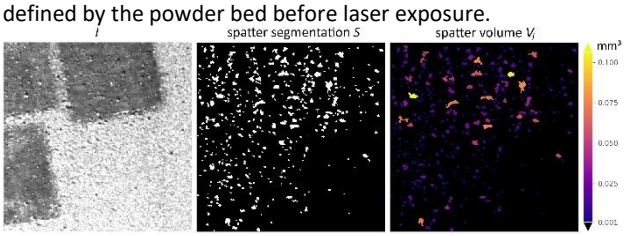

Figure 6. Intensity image I (left), binary segmentation map S (middle) and spatter volume V_i (right).

4. Experiment and empirical validation

The proposed method is verified experimentally within the scope of three build jobs. The build jobs were executed with an L-PBF machine AconityLAB from Aconity3D. AlSi10Mg was used as building material for printing geometries of simple cubes. Each build job consists of ninety-nine layers, which are split into three equally large phases. In each phase, process parameters are varied. The goal of the experiment is to verify whether a change in process parameters is visible when observing and quantifying spatter volume with the proposed technique. In all three phases, the laser power of 400 W had been used. However, the energy flow into the material is altered by using different laser scanning speeds, as indicated in table 1.

Table 1. Process parameter variation for the three phases of build job execution.

Parameter variation	Name	Energy input level
1	Standard	100 %
2	Underheated	66 %
3	Overheated	200 %

The build job consists of 7 cubes with base area of either 1 cm² or 2 cm². The cubes are rotated by 10° towards the laser trajectory direction. Also, the gas flow is altered for one build job to investigate its impact on the spatter development. The build job variations are listed in table 2. Each build job is executed and observed in-situ with the structured light system. The total spatter volume V of each layer is calculated, by summing up the individual spatter droplet volumes V_i.

Table 2. Variations of build job geometry and gas flow for the experiments. A_e is the summed part cross-section per layer.

Build job variation	Total exposed area A_e	Gas flow
1	1 400 mm²	100 %
2	1 400 mm²	70 %
3	700 mm²	100 %

$$V = \sum V_i$$

The result for each of the build job variations is plotted in the upper graph of figure 7. As the spatter development is caused by laser exposure, the spatter development can also be correlated to the laser exposure area defined in the build job A_e. The measured total spatter volume V divided by its build job laser exposure area A_e is plotted in the lower graph of figure 7.

$$V_r = V/A_e$$

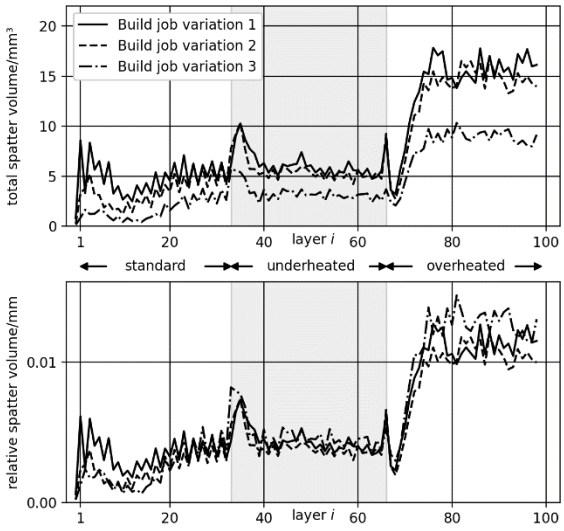

Figure 7. Spatter volume V (top) and relative spatter volume V_r (bottom).

5. Discussion of results and conclusion

The graphs in figure 7 show the measured spatter volume for different build jobs and different process parameters. All three graphs follow the same trend, which indicate a high level of reproducibility.

Looking at the temporal development of each measurement, the initial layers of each phase show divergent and fluctuating behaviour. Only around fifteen layers, the total spatter volume reaches some kind of equilibrium. The reason for this had not been investigated, however temperature effects could very well explain the phenomenon. When laser exposure begins, i.e. at the beginning of the build job, the temperature of the material rises continuously with each layer printed until the temperature reaches an equilibrium. This heating procedure is repeated when the build job phases transition, i.e. at layer 33 and layer 66. For technical reasons, the build job had to be on hold for around five minutes during this transition. During this time, the material cools down again. Different material temperatures could then cause different levels of spatter development.

The measurement of total spatter volume V indicates a strong correlation between developing spatter volume and the process condition, caused by the employed process parameters. Through quantifying spatter during manufacturing, impaired process stability is successfully detected through the measured data. However, the significance for overheating is much higher compared to underheating.

Furthermore, the relative spatter volume V_r indicates a second, strong correlation between total spatter volume and the size of the exposed area. This is expected, as spatter develops during laser exposure. This correlation also suggests some kind of build job geometry invariance, which would allow for a general application of the method.

Finally, the observed spatter distribution indicates a notable affiliation between spatter droplet trajectory and gas flow direction and intensity.

6. Operational potential of spatter detection and future work

It was shown that process monitoring based on fringe light projection to detect and quantify the concentration of spatter on the powder bed yields an indication for measuring the current process stability per layer. The reproducibility shown allow a high robustness of the measurements to be expected. The priority influences from the various process conditions could also be determined from the measured data and allow an interpretation of the measurement data in relation to the assessment of the process stability.

Nevertheless, the selected process parameters and conditions allowed for a good evaluation of the process stability. A statement in all process conditions has yet to be validated. This requires further experiments based on significantly more process parameter sets as well as different part geometries and materials in order to increase the database and to prove the interpretability of measured data even for small changes of state during the manufacturing process.

In the current state, the system acquires thirteen images per camera - seven binary patterns, four sine patterns and two reference images. With an analogue slide projector in use, the measurement or data acquisition of a single depth map takes over 15 s. The data processing takes similarly long.

To reduce data acquisition time, the total number of images used to reconstruct the three-dimensional information can be reduced. An investigation by Hexagon Technology Center GmbH has shown, that as little as four images per camera are sufficient to reconstruct a simple, primarily flat and almost two-dimensional topography as found on the powder bed. Additionally, the use of a digital projector can drastically increase the number of projected patterns per unit of time. Assuming a maximum refresh rate of 30 fps for the cameras and the projector, the theoretical data acquisition time can be as low as 133 ms ($4 \cdot 1/30$ s) per depth scan. A refresh rate of 30 fps is well within state-of-the-art performance for both components.

Equally, several ways of speeding up the data processing exist. Algorithmic optimization, the possibility of parallelization on GPUs and the ongoing development in terms of hardware performance advances result in a vast optimization potential. While data processing in a real time fashion is a realistic goal, many applications don't even depend on that and allow for delayed measurement results.

Potential applications of defect detection can be found in benchmarking process parameters as well as the assessment, maintenance and long-term monitoring of the process capability of L-PBF manufacturing machines in single-part and series production to ensure final part quality.

References

[1] Ahmad Bin Anwar, Quang-Cuong Pham 2019 *Additive Manufacturing* **22** 86-97
[2] Wischeropp T M, Emmelmann C, Brandt M and Pateras A 2019 *Additive Manufacturing* **28** 176-183
[3] zur Jacobsmühlen J, Kleszczynski S, Schneider D and Witt G 2013 *IEEE Int. Instrumentation and Measurement Tech. Conf.* 707-712
[4] Kleszczynski S, zur Jacobsmühlen J, Reinarz B, Sehrt J, Witt G and Merhof D 2014 *Improving Process Stability of LBM Systems*
[5] Zhang B, Ziegert J, Farahi F and Davies A 2016 *Additive Manufacturing* **12** 100-107
[6] Land W S, Zhang B, Ziegert J and Davies A 2015 *Procedia Manufacturing* **1** 393-403
[7] Robinson K 2004 *Pattern Recognition Letters* **25** 1759-1767
[8] Wu K, Otoo E and Shoshani A 2005 *Optimizing connected component labeling algorithms*